

Ionospheric Structures Detected by Radio Tomography during the Geomagnetic Disturbances

Vyacheslav Kunitsyn¹, Evgeniy Tereshchenko², Elena Andreeva¹,
Maksim Kozharin¹, and Marina Nazarenko¹

¹ Faculty of Physics, Lomonosov Moscow State University, Moscow, Russia

² Polar Geophysical Institute of the Russian Academy of Sciences, Murmansk, Russia

ABSTRACT

The geomagnetic disturbances deeply affect the dynamical regime of the ionosphere and cause significant variations in the ionospheric parameters. We discuss the ionospheric structures imaged by satellite radio tomography during the geomagnetically disturbed periods of solar cycles 23 and 24. Special emphasis is placed on the results from low orbiting radio tomography (LORT). Various wavelike disturbances, isolated spots of enhanced and depleted electron density, sharp wall-like density gradients, and ionospheric troughs are identified. Many LORT images in the northwestern Russia, Alaska, U.S. West Coast, and South East Asia are verified by independent methods (ionosonde measurements, radar data, etc). A series of the ionospheric features are probably associated with particle precipitation. High-orbiting RT (HORT) reconstructions based on GPS/GLONASS satellite systems help to more accurately locate the positions and trace the dynamics of the ionospheric irregularities detected by LORT.

1. INTRODUCTION

The satellite ionospheric radio tomography (RT) is an effective instrument for studying the structure and dynamics of the ionosphere. The method was developed in the early 1990s [1-4]. Even the first Russian-American Tomography Experiment has proven its viability and demonstrated its broad possibilities in reconstructing the distributions of electron density in the ionosphere. The results provided by RATE were verified by the Millstone-Hill radar data [5]. In the subsequent years, numerous RT experiments were carried out in different regions of the world under different solar and geomagnetic activity [2-4, 6-7]. These studies revealed a series of new features in the structure and dynamics of the ionosphere. Particular interest is attached to the disturbed ionosphere with strongly structured and rapidly varying distribution of electron density. RT methods are capable of imaging these ionospheric features.

2. METHOD

We focus on the ionospheric images provided by the LORT. LORT methods use dual frequency radio signals transmitted from the low-orbiting navigational satellite systems (Russian Tsikada/Parus and American Transit) and recorded by the chains of ground receivers. The inversion of phase data on the set of intersecting satellite-to-receiver rays yields almost instantaneous (on the time scale of the studied ionospheric irregularities) two-dimensional (2D) images of the ionospheric electron density above the receiving chains. The LORT resolution, typically 30-40 and 20-30 km in the horizontal and vertical directions respectively, can be improved up to 10-20 km by the allowance of the refraction of probing rays. The LORT images are in some cases effectively supported by the reconstructions provided by high-orbiting RT, which is based on the high-orbiting GNSS systems (GPS, GLONASS, etc.). Combination of LORT and HORT approaches makes it possible to suppress, to a certain degree, the individual drawbacks of these methods (essential two-dimensionality and poor spatial coverage of LORT; data incompleteness and slow satellite

motion of HORT) and to amplify their advantages (high resolution of HORT and excellent spatial and temporal coverage of HORT suitable for reconstructing the sequences of 3D ionospheric images) [6-8].

3. DATA

The data from a few LORT systems in the world provided the input to this study. Most reconstructions are based on the measurements by the Russian RT chain. It includes up to 11 Russian receivers aligned approximately with the Svalbard--Kola Peninsula--Moscow--Sochi geomagnetic meridian. At present, continuous measurements are carried out at the northern segment of the chain (Moscow--Svalbard); however, operation of the entire transcontinental chain has demonstrated its efficiency and unique coverage (the length of the chain is ~4000 km). We also processed the data from the Alaska RT chain, courtesy of the Northwest Research Associates (NWRA). The records from the United States West Coast RT chain were yet another data source. This chain was operated by Radio-Hydro-Physics LLC [9]. The structure of the equatorial ionosphere was studied from the measurements at the Low-latitude Ionospheric Tomography Network [10]. The RT processing was carried out by the phase-difference methods [11, 12], which avoids the phase uncertainty problem inherent in the ionospheric RT problems. We have processed the data for a series of the geomagnetically disturbed intervals ($K_p = 4$ to 9) of the 23rd and 24th solar cycles. Some data were analyzed jointly with HORT images and analyzed together with the radar and ionosonde data. This analysis identified a series of the ionospheric features and in some cases suggested the geophysical interpretation of the obtained RT results.

4. RESULTS

The RT images of electron density distributions during the disturbed intervals of the 23rd and 24th solar cycles revealed a broad variety of ionospheric features in the studied regions. The LORT imaging of the equatorial ionosphere during the disturbed intervals shows that the equatorial anomaly (EA) becomes fragmented and can move from its typical position in the quiet conditions. The LORT reconstructions in Figs. 1 and 2 show the electron density distribution above the Taiwan chain during the geomagnetic storm of December 2006 ($K_p = 7.7$). Wavelike disturbances are observed in the latitudinal interval of 24° - 26° . South of it, the electron density drastically drops to 0.5-0.2 the disturbed level. The two separated wavelike structure observed at 21:39UT in the core of the anomaly merge into a single maximum 17 min later at 21:56 UT.

Many LORT images of the midlatitude and subauroral ionosphere show a distinct ionization trough aligned with the geomagnetic field. The example above the Alaska RT chain is shown in Fig. 3. The ionization trough at 61° - 62° N in Fig. 4 was observed above the Russian chain during the geomagnetic storm on September 12, 2014. North of the trough, the ionosphere is structured into the wavelike disturbances in the interval of $\sim 67^\circ$ - 68° N. A very narrow depletion (~ 30 km) of ionospheric plasma is seen at about 60° N above Alaska (Fig. 5, $K_p = 5$). The example of the ionospheric trough observed during moderate geomagnetic activity ($K_p = 4.7$) above the U.S. West Coast is shown in Fig. 6. The trough is centered at $\sim 48^\circ$ - 49° N and framed on the both sides by the wavelike disturbances. The example of the ionospheric trough observed during moderate geomagnetic activity ($K_p = 4.7$) above the U.S. West Coast is shown in Fig. 6. The trough is centered at $\sim 48^\circ$ - 49° N and framed on the both sides by the wavelike disturbances.

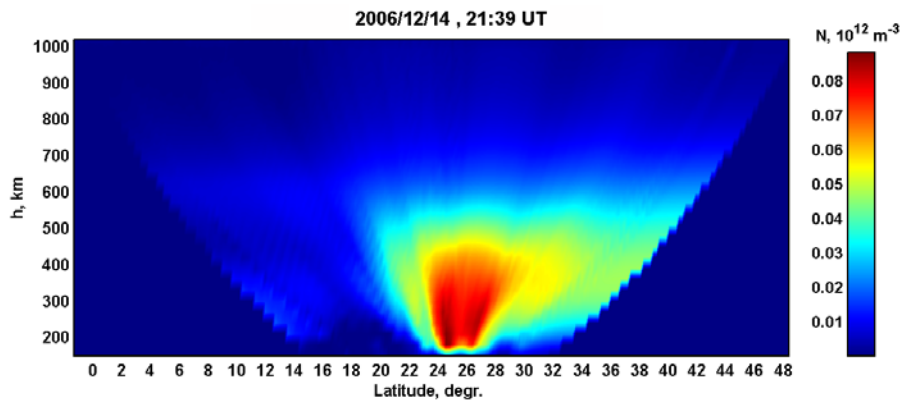


Figure 1. LORT image above the Taiwan region on December 14, 2006, 21:39UT ($K_p = 7.7$)

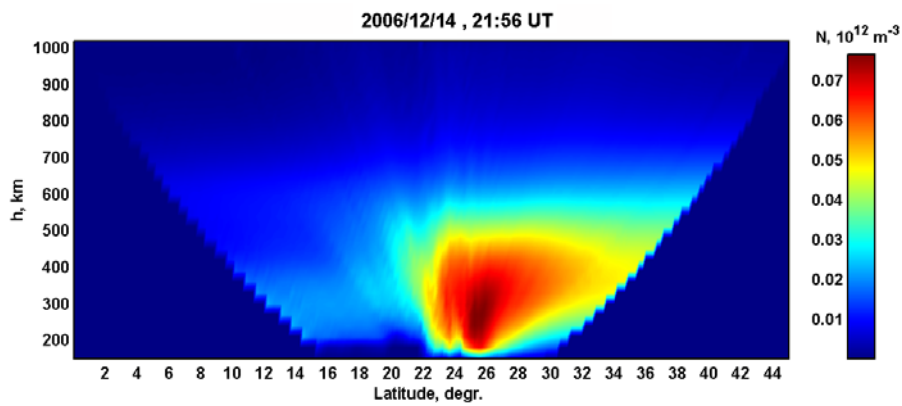


Figure 2. LORT image above the Taiwan region on December 14, 2006, 21:56UT ($K_p = 7.7$)

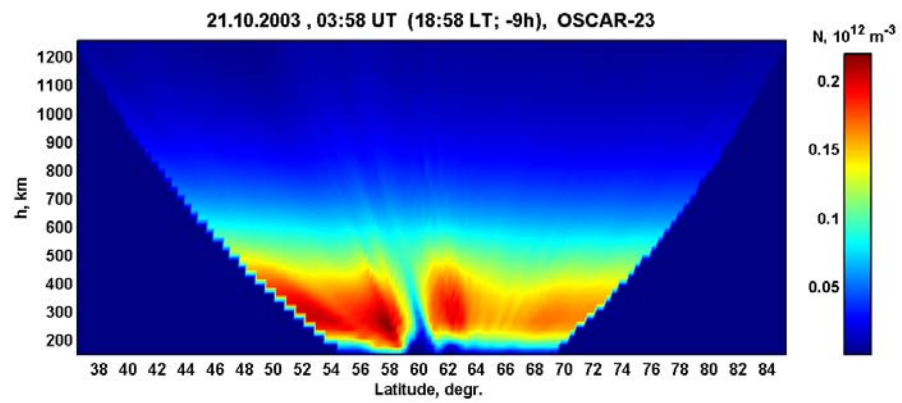


Figure 3. LORT image above Alaska on October 21, 2003, 03:58UT ($K_p = 4.7$)

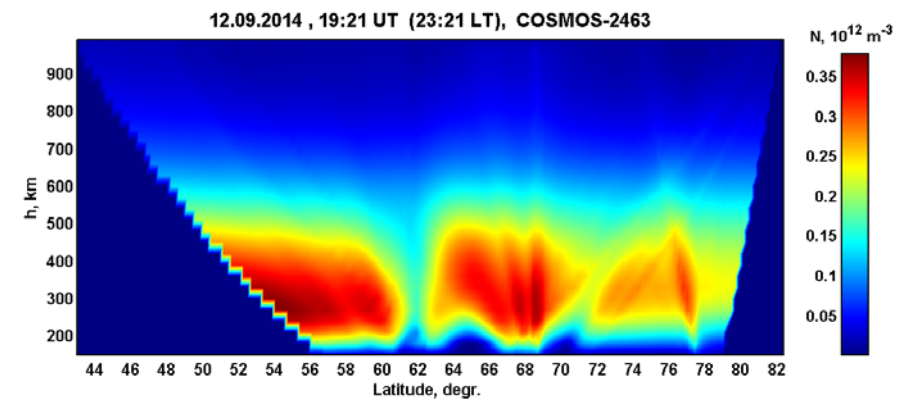


Figure 4. LORT image above Russian RT chain on September 9, 2014, 19:21UT ($K_p = 4.7$)

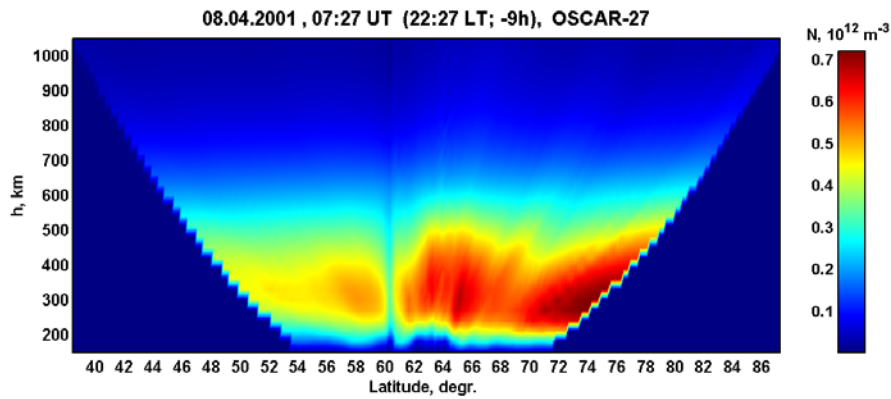


Figure 5. LORT image above Alaska on April 8, 2001, 07:27UT ($K_p=5$)

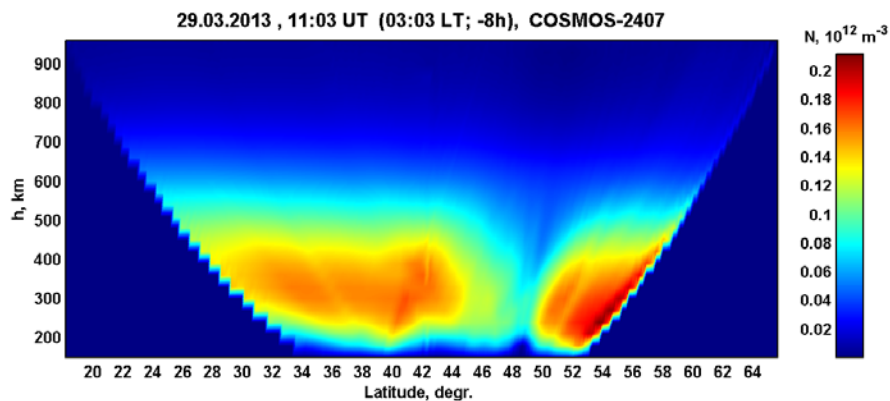


Figure 6. LORT image above the U.S. West Coast on March 29, 2013, 11:03UT ($K_p=4.7$)

The LORT images demonstrate a broad variety of the shapes and positions of the troughs in the ionosphere during the geomagnetically active periods. As the geomagnetic disturbances become more intense, a trough may move equatorwards, its polar wall may change its slope and configuration; the plasma on either or both sides of the trough is often structured into the wavelike patterns.

Wavelike structures are quite common in both the weakly and strongly disturbed ionosphere. The example in Fig. 7 shows the wave disturbances observed in the quiet ionosphere ($K_p < 1$) above the Russian chain on February 23, 2012. The geometry of the experiment and characteristic slopes of the waves suggest their northward motion.

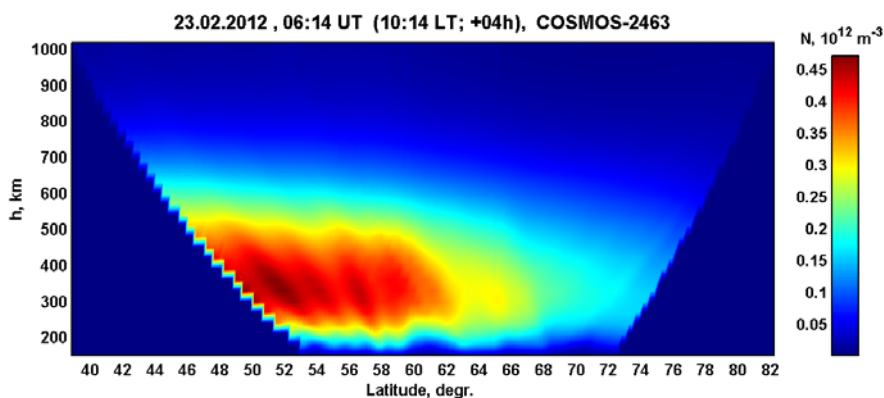


Figure 7. LORT image above the Russian RT chain on February 23, 2012, 06:14UT ($K_p < 1$)

The example of the ionospheric structure above the Russian RT system and RT chain in Alaska during the disturbed interval at $\sim 5:40$ UT on July 27, 2004 ($K_p = 7.3$) is shown in

Fig.8. The American chain fell in the evening sector, and the Russian chain, in the morning sector. The wavelike structures are observed in the ionosphere above the both chains.

The strongly disturbed ionosphere above Alaska (April 11, 2001, $K_p = 7$, Fig. 9) has a trough in the interval of $59\text{--}60^\circ\text{N}$, which is farther north followed by the periodical structures observed in the interval $60\text{--}66^\circ$. A spot of enhanced ionization is present in the northernmost segment of the image.

Generally, the LORT reconstructions revealed various wave structures at different latitudes during the geomagnetic disturbances. The depth of modulation and absolute values of the ionospheric electron density may reach quite high levels. The wave disturbances in some images occur as a wave train spanning a few degrees to a few tens of degrees in latitude. The wave structures during the high geomagnetic activity are typically complicated by the variations in the bottom height of the disturbed ionospheric layer, in the slopes of the plasma wave structures, their width and vertical extent within the wave train.

The LORT images of the disturbed ionosphere often show multi-extrema distributions of electron density, with the areas of enhanced and depleted plasma in the form of isolated spots or a series of the spots of different lengths, shapes, and intensity. Figure 10 presents the example. This density distribution was observed above the Russian RT chain at 21:25 UT on October 30, 2003, during the strongest Halloween storm with $K_p = 9$. This phenomenon has been extensively studied by many authors. The LORT and HORT imaging, ionosonde measurements, and observations by the EISCAT Svalbard and mainland (Tromso) radars [13, 14] established a complicated highly structured electron density distribution above the high-latitude Scandinavia regions and northwestern Europe in the evening on October 30, 2003.

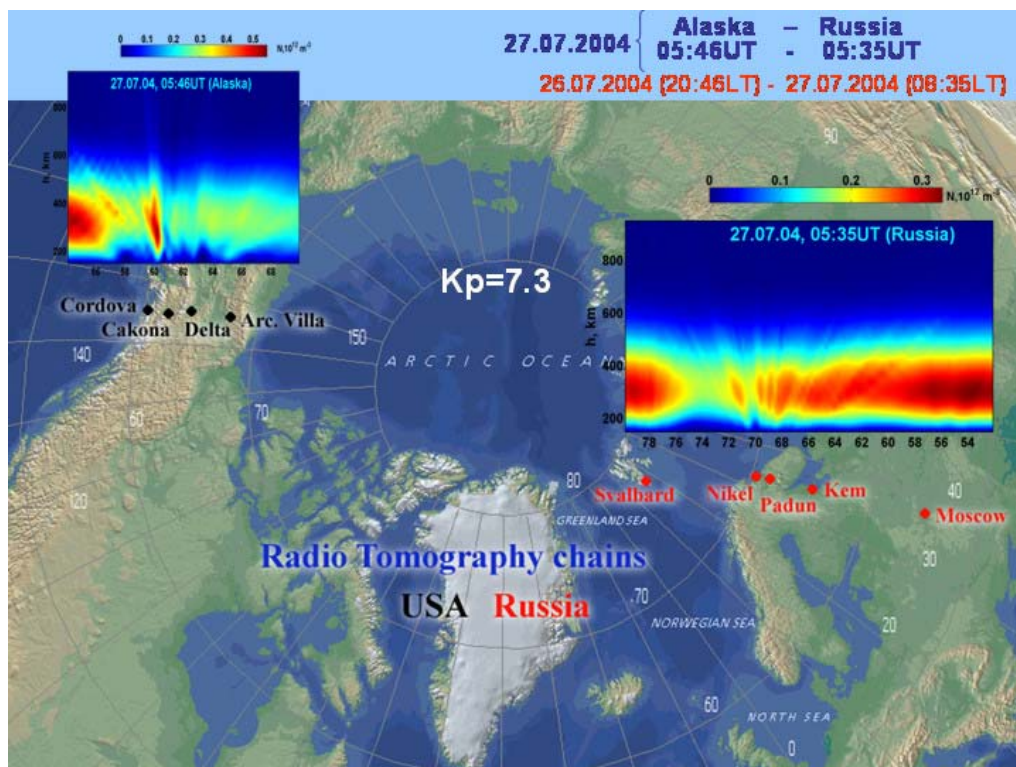


Figure 8. LORT images of the ionosphere above the Russian and Alaska RT chains on July 27, 2004, at 05:35 UT and 05:46 UT, $K_p = 7.3$.

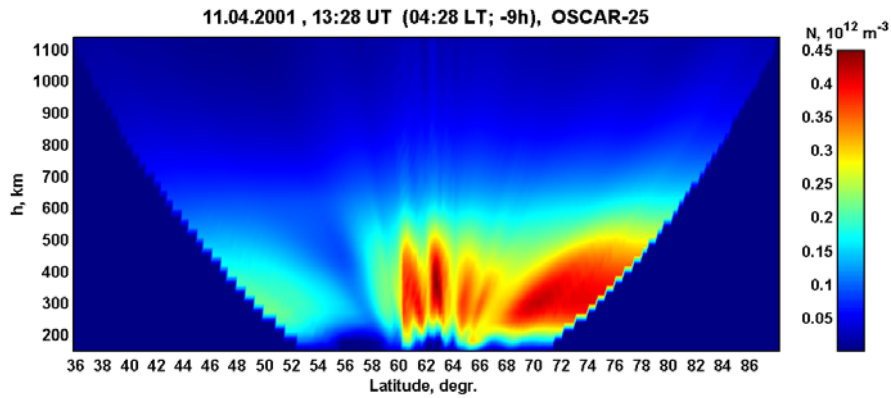


Figure 9. LORT image above the Alaska on April 11, 2001, 13:28 UT ($K_p = 7$)

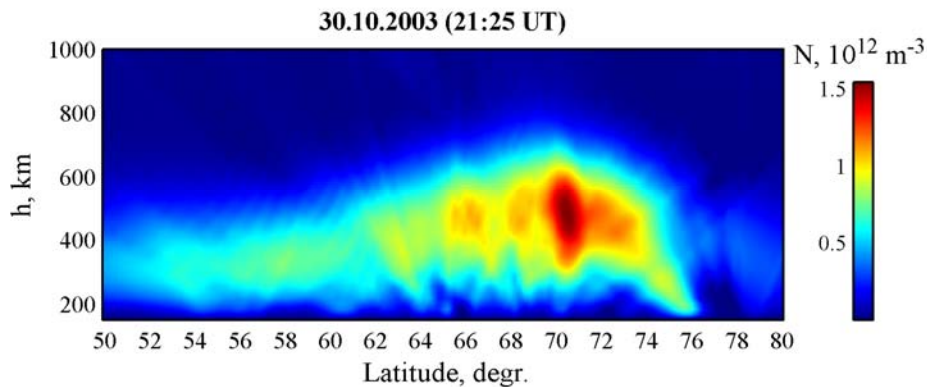


Figure 10. LORT image above the Russian RT chain on October 30, 2003, 21:25 UT ($K_p=9$)

Based on the HORT images, we traced the further motion of this plasma structure as it leaved the Svalbard area and entered the European sector. The highly structured plasma was moving above Europe from the Kola Peninsula to the British Isles. It produced extremely high density values in the nighttime ionosphere, which were commensurate with the typical daytime concentrations. The measurements by the European ionosondes support the RT results [13].

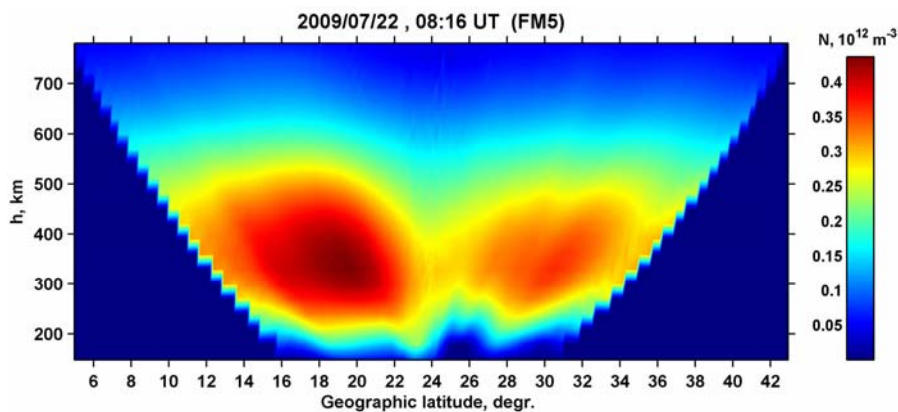


Figure 11. LORT image of the ionosphere in the South East Asia on July 22, 2009, 8:16 UT. $K_p = 5$.

The electron density distributions in the ionosphere during the geomagnetic disturbances can be strongly affected by precipitation. These effects are often observed in the RT images. The RT reconstructions in the Southeast Asia revealed the effect of ionization of the equatorial ionosphere by quasi trapped energetic (> 30 keV) electrons. It was shown that, although these electrons have small ionization cross-section, they strongly enhance below the

radiation belts (due to their long persistence in the forbidden zones) and produce additional ionization in the topside ionosphere during the storms driven by the coronal-mass ejections and recurrent storms. This effect can be observed during the positive phase of major storms and during moderate storms as well [15, 16]. This is illustrated by Fig. 11. The LORT image of the ionosphere in the South-East Asia during the magnetic storm of July 22, 2009 at 8:16UT reveals the core of EA oriented along the magnetic field and a weaker maximum north of the core. The comparison of this LORT image with particle precipitation data shows that this structure is due to the ionization by quasi-trapped energetic electrons at a height of 300-600 km, which may greatly contribute to the ionization of the subequatorial ionosphere up to the latitudes of 35° [16].

5. CONCLUSIONS

The LORT images of the ionosphere in Russia, North America, and South East Asia during the periods of geomagnetic disturbances show a great variety of density features. The reconstructions revealed the ionospheric trough with different intensity and shape, which migrated with the enhancement and decay of geomagnetic disturbances. Various complicated density distributions with numerous spots of increased and decreased ionization are identified. Wavelike structures are present. In some cases, it is possible to locate the origin of the wave disturbance and to trace the evolution of the wavelike structure. The effect of additional ionization of subequatorial ionosphere by quasi trapped energetic electrons is revealed. Combination of HORT and LORT methods supported by the other ground- and satellite-based observations will probably shed the new light on the processes controlling the distributions of ionospheric plasma at different latitudes during the geomagnetic disturbances.

6. ACKNOWLEDGMENTS

We are deeply grateful to NWRA, Radio-Hydro-Physics LLC, and Center for Space and Remote Sensing Research at the National Central University, Taiwan for providing the data for LORT analysis. The work was supported Russian Science Foundation (grant no. 14-17-00637). The part of the analysis of the structure of the ionosphere by the RT methods was supported by the Russian Foundation for Basic Research (grant no. 13-05-01122).

REFERENCES

1. Kunitsyn, V.E, and Tereschenko, E.D., Radiotomography of the Ionosphere, IEEE Antennas and Propagation Magazine (1992). 34, 22-32.
2. Kunitsyn, V.E., and Tereshchenko, E.D., Ionospheric Tomography, Berlin: Springer; (2003).
3. Pryse S.E. Radio tomography: A new experimental technique, *Surv. Geophys.* (2003), 24, doi:10.1023/A:1022272607747
4. Bust, G.S., Mitchell, C.N. History, current state, and future directions of ionospheric imaging, *Rev. Geophys.* (2008), RG1003, doi:10.1029/2006RG000212
5. Foster, J, Buonsanto, M, Holt, J, Klobuchar, J, Fougere, P, Pakula, W, Raymund, T, Kunitsyn, V.E, Andreeva, E.S, Tereshchenko, E.D, and Khudukon, B.Z., Russian-American Tomography Experiment. *Int. J. Imag. Sys. Technol.* (1994), 5, 148-159.
6. Kunitsyn VE, Tereshchenko ED, Andreeva ES, Nesterov IA. Satellite radio probing and radio tomography of the ionosphere. *Uspekhi Fizicheskikh Nauk*, (2010), 180(5) 548-553

7. Kunitsyn, V.E., Andreeva, E.S., Nesterov, I.A., Padokhin, A.M. Ionospheric Sounding and Tomography by GNSS. In book: *Geodetic Sciences - Observations, Modeling and Applications*, S. Jin (ed.), InTech. (2013), 223-252, ISBN 978-953-51-1144-3.
8. Kunitsyn, V.E, and Nesterov, I.A., GNSS radio tomography of the ionosphere: The problem with essentially incomplete data. *Adv. Space Res.* (2011), 47, 1789-1803.
9. V. Kunitsyn, E. Andreeva, I. Nesterov, A. Padokhin, D. Gribkov, and D.A. Rekenhtaler. Earthquake prediction research using radio tomography of the ionosphere. In *Universe of Scales: From Nanotechnology to Cosmology*, vol. 150 of *Springer Proceedings in Physics*, pages 109–132. Springer International Publishing New York, United States, 2014
10. Andreeva, E.S, Franke, S.J, Yeh, K.C, and Kunitsyn, V.E. Some features of the equatorial anomaly revealed by ionospheric tomography, *Geophys. Res. Lett.* (2000), 27, 2465-2458.
11. Andreeva, E.S, Kunitsyn, V.E, and Tereshchenko, E.D., Phase difference radiotomography of the ionosphere. *Annales Geophysicae* (1992), 10, 849-855.
12. Kunitsyn, V.E, Andreeva, E.S, Razinkov, O.G, and Tereschhenko, E.D., Phase and phase-difference ionospheric radiotomography. *International Journal of Imaging Systems and Technology* (1994), 5(2), 128-140.
13. Kunitsyn, V.E, Kozharin, M.A, Nesterov, I.A, and Kozlova, M.O., Manifestations of helio-geophysical disturbances in October, 2003 in the ionosphere over West Europe from GNSS data and ionosonde measurements. *Moscow University Physics Bulletin* (2004), 59(6), 68-71.
14. P. Yin, C.N. Mitchell, P. Spencer, I. McCrea, and T. Pedersen, A multi-diagnostic approach to understanding high-latitude plasma transport during the Halloween 2003 storm, *Ann. Geophys.* (2008), 26, 2739–2747
15. Suvorova, A.V., Dmitriev A.V., Tsai, L.-C., Kunitsyn, V.E., Andreeva, E.S., Nesterov, I A., Lazutin L.L. TEC evidence for near-equatorial energy deposition by 30 keV electrons in the topside ionosphere, *J. Geophys. Res.: Space Physics* (2013), 118, doi:10.1002/jgra.50439
16. Suvorova, A. V., C.-M. Huang, H. Matsumoto, A. V. Dmitriev, V. E. Kunitsyn, E. S. Andreeva, I. A. Nesterov, and L.-C. Tsai, Low-latitude ionospheric effects of energetic electrons during a recurrent magnetic storm, *J. Geophys. Res. Space Physics* (2014), 119, doi:10.1002/2014JA020349.